Title

Coupling Pressure Sensing with Optical Coherence Tomography to Evaluate the Internal Nasal Valve.

Journal

The Annals of otology, rhinology, and laryngology, 130(2)

ISSN

0003-4894

Authors

Hakimi, Amir A
Sharma, Giriraj K
Ngo, Tuan
et al.

Publication Date

2021-02-01

DOI

10.1177/0003489420944199

Annals of Otology, Rhinology & Laryngology
2021, Vol. 130(2) 167–172

DOI: 10.1177/0003489420944199
journals.sagepub.com/home/aor
SAGE

Coupling Pressure Sensing with Optical Coherence Tomography to Evaluate the Internal Nasal Valve

Amir A. Hakimi, BS[1], Giriraj K. Sharma, MD, MS[1,2], Tuan Ngo, MD[1], Andrew E. Heidari, PhD[1,2], Christopher D. Badger, MD[1], Prem B. Tripathi, MD, MPH[1,2], Ellen M. Hong, BA[1], Zhongping Chen, PhD[3], and Brian J. F. Wong, MD, PhD[1,2,3]

Abstract

Purpose: To evaluate endoscopic long-range optical coherence tomography system combined with a pressure sensor to concurrently measure internal nasal valve cross-sectional area and intraluminal pressure.

Methods: A pressure sensor was constructed using an Arduino platform and calibrated using a limiter-controlled vacuum system and industrial absolute pressure gauge. Long-range optical coherence tomography imaging and pressure transduction were performed concurrently in the naris of eight healthy adult subjects during normal respiration and forced inspiration. The internal nasal valve was manually segmented using Mimics software and cross-sectional area was measured. Internal nasal valve cross-sectional area measurements were correlated with pressure recordings.

Results: Mean cross-sectional area during forced inspiration was 6.49 mm^2. The mean change in pressure between normal respiration and forceful inspiration was 12.27 mmHg. The direct correlation between pressure and cross-sectional area as measured by our proposed system was reproducible among subjects.

Conclusions: Our results demonstrate a direct correlation between internal nasal valve cross-sectional area and nasal airflow during inspiration cycles. Endoscopic long-range optical coherence tomography coupled with a pressure sensor serves as a useful tool to quantify the dynamic behavior of the internal nasal valve.

Keywords

nasal valve, optical coherence tomography, intranasal pressure, airway obstruction, internal nasal valve

Introduction

The internal nasal valve (INV) is the narrowest segment of the nasal cavity bound by the upper lateral cartilages, dorsal septum, and inferior turbinate.[1] High velocity airflow entering this constricted space generates considerable pressure differentials that contribute to sidewall collapse.[2] This nasal valve collapse is associated with symptomatic nasal airway obstruction (NAO), a condition that is estimated to affect over 60% of the United States geriatric population.[3] Consequently, facial plastic surgeons and rhinologists have long searched for a simple and clinically accessible technique to objectively evaluate the nasal airway.

The most recent clinical consensus statement by Rhee et al concluded that there is currently no single gold standard test to diagnose NAO.[4] Rather, diagnosis is primarily based on a patient's history and physical examination. This is primarily due to discrepancies between subjective patient-reported symptoms of nasal obstruction and objective clinical examination measurements. However, recent studies utilizing computational fluid dynamics (CFD) have identified nasal airflow and mucosal cooling as reliable correlates to subjective nasal patency.[5-8] Although classic rhinomanometry provides valuable measurements of nasal airflow, it is limited in clinical value without correlative visualization of the underlying obstructive anatomy. As such, there is a need

[1]Beckman Laser Institute & Medical Clinic, University of California - Irvine, CA, USA
[2]Department of Otolaryngology—Head & Neck Surgery, University of California - Irvine, CA, USA
[3]Department of Biomedical Engineering, University of California - Irvine, CA, USA

Corresponding Author:
Brian J. F. Wong, MD, PhD, Beckman Laser Institute, 1002 Health Sciences Road, Irvine, CA 92697, USA.
Email: bjwong@uci.edu

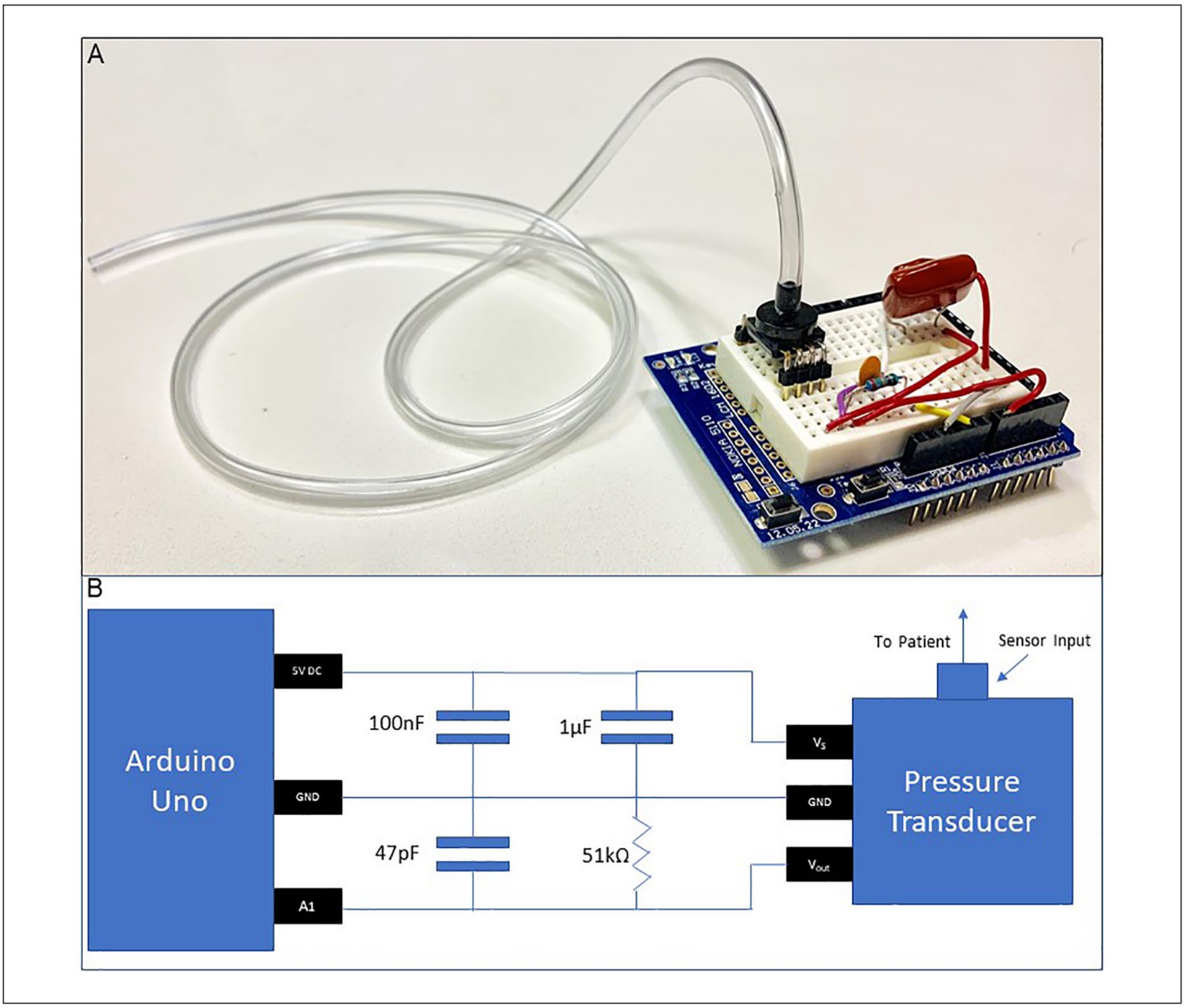

Figure 1. Pressure sensor hardware, including (A) Arduino, breadboard, and tubing, (B) breadboard schematic.
A1 = analog input port 1 on the Arduino circuit. Measures the output voltage (V_{out}) on the pressure transducer indicating a change in pressure.
V_s = Input power port for pressure transducer. Requires a 5 Volt DC input power for the pressure transducer to operate.
V_{out} = Output voltage of the pressure transducer that varies based on the measured pressure.
5 V DC = Voltage output from the Arduino circuit used to power the pressure transducer.

for a comprehensive diagnostic tool to both visualize and assess airflow within the nasal cavity.

Optical Coherence Tomography is a near infrared, non-contact imaging modality that acquires depth-resolved information of tissues at a micron scale resolution.[9] The efficacy of endoscopic long-range optical coherence tomography (LR-OCT) to precisely quantify INV geometry in healthy patients has been previously established.[10-12] Herein, we describe the development and feasibility of an LR-OCT system coupled with a calibrated pressure sensor to image the INV and simultaneously record intraluminal pressure during normal respiration and forced inspiration.

Methods

Pressure Sensor

An Arduino Uno microcontroller (Arduino LLC., Scarmagno, Italy) was used to build a pressure sensing device. A breadboard (Figure 1A) was utilized for rapid prototyping of the necessary circuit to optimize gain and frequency response of the pressure sensor (Figure 1B). A piezoelectric sensor (MPXV6115V, Freescale Semiconductor) was attached to the breadboard (Figure 1C). A 10 cm flexible clear tubing (Grainger Inc., Lake Forest, Illinois) was attached onto the sensor that had an

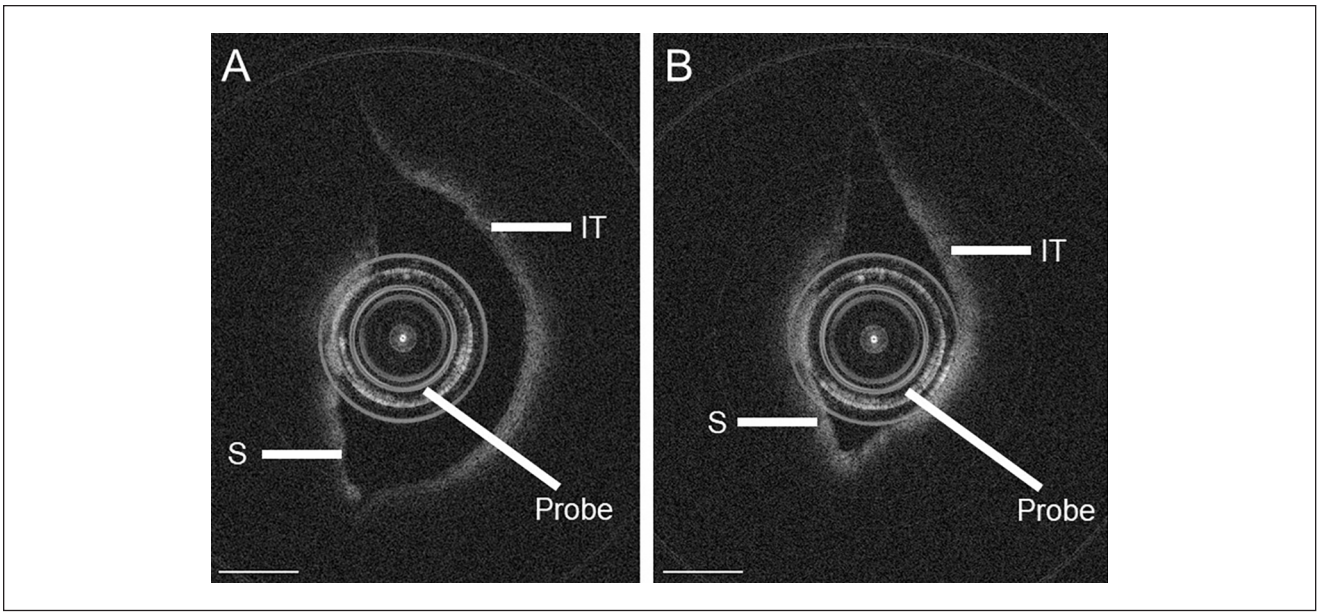

Figure 2. OCT images of the INV during (A) normal inspiration and (B) forced inspiration.
Abbreviations: IT, inferior turbinate; S, septum.
Scale = 1 mm.

approximate inner diameter of 1 mm. A 5 V battery was used to power the device and reduce noise. The Arduino IDE Software codes were programmed in C++ language. Software converted the voltage signal from the sensor to pressure (mmHg).

Sensor Calibration

The pressure sensor was validated against a continually calibrated industrial absolute pressure gauge in an aerodynamic research laboratory. There was a one-to-one linear correlation ($r^2 = 0.9997$) in the working range of −863 mmHg (115 kPa) to 0 mmHg (0 kPa). Thereafter, the device was consistently calibrated using a classic U-tube water manometer (Grainger Inc., Lake Forest, Illinois).

Clinical Imaging

An endoscopic long-range swept source Fourier domain optical coherence tomography system was used which has been previously described.[12,13] Eight healthy adult subjects without history of NAO, allergic rhinitis, recurrent sinusitis, or previous nasal surgery underwent LR-OCT imaging and pressure measurements of the INV. Imaging was performed in a single nasal vault on seated, awake individuals. The LR-OCT probe and pressure sensor were affixed to one another and manually advanced by the operator, in tandem. The septum was readily visualized upon insertion into the nasal cavity. The probe was advanced further until the anterior head of the inferior turbinate was visualized. This was the key landmark for identifying the INV as it is not present in the nasal vestibule. Once visualized, the probe was held in place for imaging and pressure acquisition (Figure 2). Volumetric spiral scan data in addition to static two-dimensional OCT images were acquired in real-time with concurrent image display. All software was coded in C++ operating on a Windows 7 platform. OCT probes were encased in a transparent and sterilized fluorinated ethylene propylene sheath (Zeus, Orangeburg, SC). These single-use sheaths were heat-sealed with a butane lighter. Measurements were obtained during normal respiration and forced inspiration.

Continuous spiral scanning from the nasopharynx produced about 500 raw images for each OCT data set. OCT data were transformed from Cartesian to polar coordinates in the Matlab software (MathWorks, Natick, MA). Mimics software (Materialise, Leuven, Belguim) was used to manually segment the INV and measure cross-sectional area (CSA).

Results

Eight healthy subjects underwent simultaneous LR-OCT imaging and intranasal pressure measurements during normal respiration and forced inspiration (Figure 3). Five participants were female, and three were male. Six (four female and two male) subjects were Asian and two (one female and one male) were Caucasian. The device was safe, minimally invasive, and well-tolerated in subjects without the need for local anesthesia or sedation. There

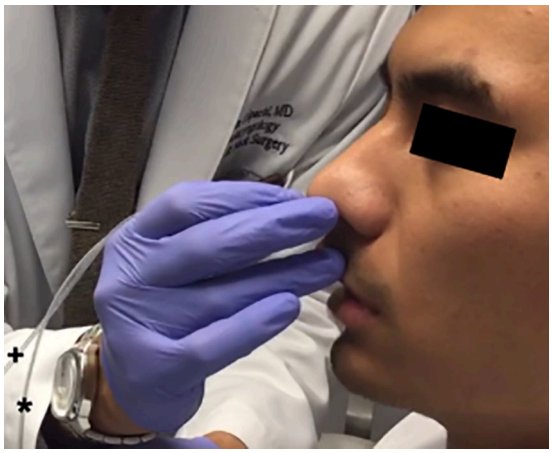

Figure 3. The OCT probe (*) and pressure sensor (+) were affixed to one another and inserted in tandem into the nasal cavity until landmarks of the internal nasal valve were visualized on OCT imaging.

were no imaging-related complications. It took approximately 15 seconds to insert the probe and identify the INV based on anatomical landmarks, and an additional approximately 30 seconds to acquire the data and remove the probe from each participant.

The mean CSA during normal and forced inspiration were 11.7 mm^2 and 6.49 mm^2, respectively. The mean change in pressure between normal respiration and forceful inspiration was 12.27 mmHg (range: 3.83 mmHg-22.19 mmHg). During forced inspiration, there was a decrease in intraluminal pressure with a corresponding decrease in CSA. This trend was reproduced in all participants (Figure 4).

Discussion

In this study, we introduced the development and utility of an endoscopic LR-OCT system coupled with a pressure sensor to concurrently measure the dynamic changes in INV behavior. Specifically, we identified a reproducible, direct correlation between CSA and intraluminal pressure, as expected. Our data supports the concept that pressure differentials in the INV created by inspiration lead to a reduction in INV CSA, and accordingly sidewall collapse. The mean CSA under forced inspiration was found to be 6.49 mm^2 which correlates well with previous values estimating forced inspiration INV CSA using OCT ($6.3 \pm 2.5\ mm^2$).[11]

One of the primary difficulties in assessing NAO stems from limitations in existing diagnostic tools.[14-17] Nasal endoscopy and the Cottle maneuver are subjective techniques with broad examiner variability. Moreover, two-dimensional images of INV CSA obtained with endoscopy or radiographic imaging poorly estimate the actual complex three-dimensional INV geometry.[18] Acoustic rhinometry provides some information on geometry without measuring airflow, but is limited in cases of severe constriction and in voluminous paranasal sinuses with large ostia.[19,20] Rhinomanometry measures nasal airflow resistance, but cannulation alters flow parameters profoundly. Our proposed technology overcomes these limitations, permitting bedside measurements of two fundamental variables: INV structural geometry and pressure change.

The LR-OCT system allows for more objective visualization of the INV compared to endoscopy as it displays surface contour information, whereas two-dimensional digital images acquired using an endoscope rely upon an operator to estimate geometry based upon a two-dimensional projection of a true three-dimensional surface. LR-OCT allows for enhanced anatomical visualization to distinguish among septal, turbinate, and sidewall causes of NAO. Moreover, the system allows for three-dimensional visualization in real-time, allowing clinicians to evaluate dynamic changes of the INV's structural framework during maneuvers such as forced inspiration. The linked pressure sensor provides concurrent manometric measurements which offer insight onto airflow and thus nasal cavity function. In tandem, nasal airflow disruptions identified with the pressure sensor can be instantaneously correlated with sites of structural weakness seen on endoscopic LR-OCT imaging. These measurements can then aid in initial diagnosis, surgical planning, and post-operative assessment of NAO. And potentially with serial imaging gates to the respiratory cycle, this system may distinguish both internal and external nasal valve collapse.

An understanding of INV geometry and intraluminal pressure is critical to assessing the work of breathing localized at the INV. Fundamentally, it is the energy expenditure required to breathe that is problematic for patients experiencing NAO. Nasal valve collapse occurs as pressure overcomes the weak nasal sidewall, resulting in increased energy consumption. A similar concept is present in pulmonary function testing. Our results demonstrate the correlation between pressure and area which may serve as a proxy for energy expenditure, or at least energy consumed by deformation of the lateral wall. Future work, however, should focus on comparing intraluminal pressure changes to INV volume which would provide information on nasal compliance. This would require the use of a more sophisticated imaging probe, but would offer insight into the work of breathing from the nasal airway similar to flow-volume loops used in pulmonary function testing.

Our described diagnostic tool is not without limitations. Excess turbid mucus in the nasal cavity can cause a drop-off in signal intensity, and thus reduce OCT image quality.[21] Additionally, this study is preliminary in nature and included a small sample of healthy volunteers. Nevertheless, even among the healthy participants, we

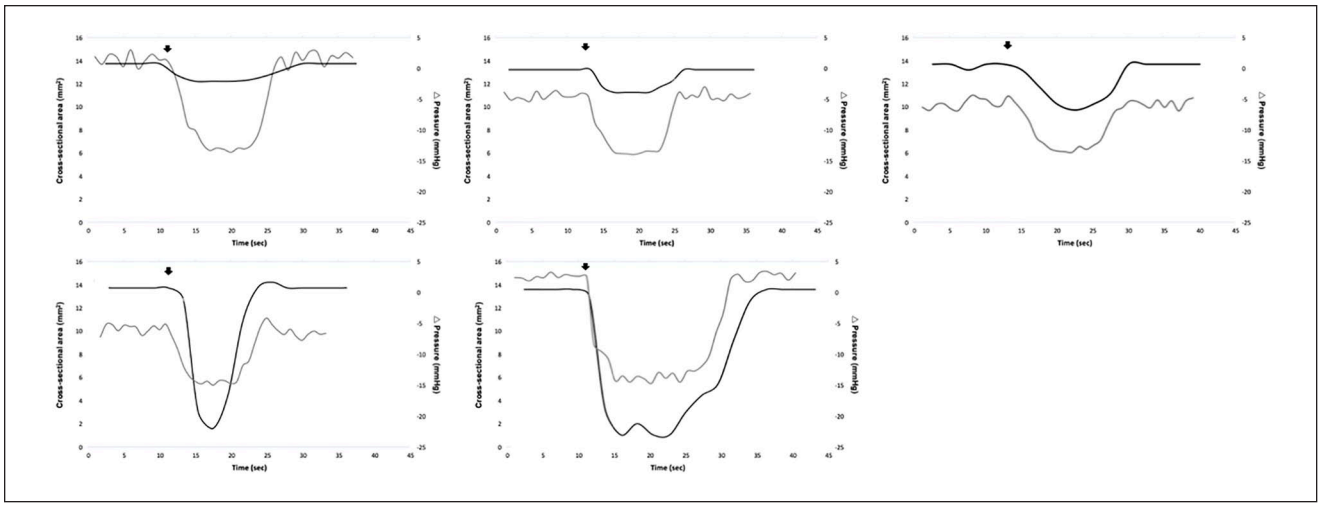

Figure 4. Sample plots of measured changes in CSA (mm^2) and pressure (mmHg) during a single forced inspiration among five participants.

found variability in pressure changes between normal and forced inspiration. This is likely due to differences in the anatomy and structural support of the INV between participants. Cem Miman et al previously classified six different INV configurations among 124 patients without nasal obstruction, each of which may result in a varied pressure change during normal and forced inspiration.[22] Moreover, we hypothesize that patients with weaker structural support of their INV will experience greater pressure differences during forced inspiration due to increased likelihood of INV collapse. Finally, since the OCT system was specially constructed, it is comparatively expensive. Despite these limitations, we hope that the demonstrated feasibility of this device will motivate further work to refine the technology and lessen costs.

Future investigations are underway to correlate the LR-OCT-intraluminal pressure measurements with other clinical examination findings, patient symptomatology, and quality-of-life scores before and after appropriate treatment. We ultimately aim to characterize normal versus abnormal intraluminal pressure values and OCT images among a large sample of both healthy and pathologic patients, respectively. Once these values are known, they may aid in objective NAO diagnosis and subsequent surgical planning.

Conclusion

LR-OCT imaging in tandem with pressure sensing is an effective and practical combined imaging and manometry adjunct to assess the effect of airflow on INV geometry. This may ultimately assist surgeons in determining the precise etiology of NAO and guide surgical management decisions.

Declaration of Conflicting Interests

The author(s) declared no potential conflicts of interest with respect to the research, authorship, and/or publication of this article.

Funding

The author(s) received no financial support for the research, authorship, and/or publication of this article.

Ethics approval

This study was given exemption status from the Institutional Review Board of the University of California – Irvine.

Consent to participate

Informed consent was obtained from all individual participants included in the study.

Consent to publish

Volunteers signed informed consent regarding publishing their data and photographs.

ORCID iDs

Amir A. Hakimi https://orcid.org/0000-0002-5675-5758

Giriraj K. Sharma https://orcid.org/0000-0002-3249-4864

References

1. Fattahi T. Internal nasal valve: significance in nasal air flow. *J Oral Maxillofac Surg*. 2008;66(9):1921-1926.
2. Tripathi PB, Elghobashi S, Wong BJF. The myth of the internal nasal valve. *JAMA Facial Plast Surg*. 2017;19(4): 253-254.
3. Clark DW, Del Signore AG, Raithatha R, Senior BA. Nasal airway obstruction: prevalence and anatomic contributors. *Ear Nose Throat J*. 2018;97(6):173-176.

4. Rhee JS, Weaver EM, Park SS, et al. Clinical consensus statement: diagnosis and management of nasal valve compromise. *Otolaryngol Head Neck Surg*. 2010;143(1):48-59.
5. Sullivan CD, Garcia GJ, Frank-Ito DO, Kimbell JS, Rhee JS. Perception of better nasal patency correlates with increased mucosal cooling after surgery for nasal obstruction. *Otolaryngol Head Neck Surg*. 2014;150(1):139-147.
6. Kimbell JS, Frank DO, Laud P, Garcia GJ, Rhee JS. Changes in nasal airflow and heat transfer correlate with symptom improvement after surgery for nasal obstruction. *J Biomech*. 2013;46(15):2634-2643.
7. Zhao K, Jiang J, Blacker K, et al. Regional peak mucosal cooling predicts the perception of nasal patency. *Laryngoscope*. 2014;124(3):589-595.
8. Shadfar S, Shockley WW, Fleischman GM, et al. Characterization of postoperative changes in nasal airflow using a cadaveric computational fluid dynamics model. *JAMA Facial Plast Surg*. 2014;16(5):319-327.
9. Huang D, Swanson EA, Lin CP, et al. Optical coherence tomography. *Science*. 2991;254(5035):1178-1181.
10. Englhard AS, Wiedmann M, Ledderose GJ, et al. Imaging of the internal nasal valve using long-range Fourier domain optical coherence tomography. *Laryngoscope*. 2015;126(3): E97-E102.
11. Englhard AS, Wiedmann M, Ledderose GJ, et al. In vivo imaging of the internal nasal valve during different conditions using optical coherence tomography. *Laryngoscope*. 2018;128(3):E105-E110.
12. Jing J, Zhang J, Loy AC, Wong BJ, Chen Z. High-speed upper-airway imaging using full-range optical coherence tomography. *J Biomed Opt*. 2012;17(11):110507.
13. Vlogger V, Sharma GK, Jing JC, et al. Long-range Fourier domain optical coherence tomography of the pediatric subglottis. *Int J Pediatr Otorhinolaryngol*. 2015;79(2): 119-126.
14. Apaydin F. Nasal valve surgery. *Facial Plast Surg*. 2011;27(2):179-191.
15. Fischer H, Gubisch W. Nasal valves – importance and surgical procedures. *Facial Plast Surg*. 2006;22(4):266-280.
16. Yoo DB, Jen A. Endonasal placement of spreader grafts: experience in 41 consecutive patients. *Arch Facial Plast Surg*. 2012;14(5):318-322.
17. Cho GS, Kim JH, Jang YJ. Correlation of nasal obstruction with nasal cross-sectional area measured by computed tomography in patients with nasal septal deviation. *Ann Otol Rhinol Laryngol*. 2012;121(4):239-245.
18. Bhatia DDS, Palesy T, Ramli R, et al. Two-dimensional assessment of the nasal valve area cannot predict minimum cross-sectional area or airflow resistance. *Am J Rhinol Allergy* 2016; 30(3):190-194.
19. Cankurtaran M, Celik H, Cakmak O, Ozluoglu LN. Effects of the nasal valve on acoustic rhinometry measurements: a model study. *J Appl Physiol*. 2003;94(6): 2166-2172.
20. Cakmak O, Celik H, Cankurtaran M, Ozluoglu LN. Effects of anatomical variations of the nasal cavity on acoustic rhinometry measurements: a model study. *Am J Rhinology*. 2005;19(3):262-268.
21. Lazarow FB, Ahuja GS, Loy AC, et al. Intraoperative long range optical coherence tomography as a novel method of imaging the pediatric upper airway before and after adenotonsillectomy. *Int J Pediatr Otorhinolaryngol*. 2015;79(1): 63-70.
22. Cem Miman M, Deliktas H, Ozturan O, Toplu Y, Akarçay M. Internal nasal valve: revisited with objective facts. *Otolaryngol Head Neck Surg*. 2006;134(1):41-47.